Electronic Supplementary Information

Non-interacting, sp2 carbon on ferroelectric lead zirco-titanate: towards graphene synthesis on ferroelectrics in ultrahigh vacuum

*Nicoleta G. Apostol,[a] George A. Lungu,[a] Ioana C. Bucur,[a,b] Cristian A. Tache,[c] Luminiţa Hrib,[a] Lucian Pintilie,[a] Dan Macovei,[a] and Cristian Mihail Teodorescu[a]**

[a]*National Institute of Materials Physics, Atomiştilor 405A, 077125 Măgurele-Ilfov, Romania*
[b]*University of Bucharest, Faculty of Physics, Atomiştilor 405, 077125 Măgurele-Ilfov, Romania*
[c]*University of Trieste, Department of Physics, Via Valerio 2 - 34127 Trieste Italy*

*corresponding author, e-mail teodorescu@infim.ro

SI-1. More experimental details and photoemission overview scans

Description of experiments: A first series of experiments was aimed to synthesize by chemical vapor deposition (CVD) carbon (graphene, Gr) layers on $Pb(Zr,Ti)O_3$ (PZT) grown on $SrRuO_3/SrTiO_3(001)$ (SRO/STO). Ethylene (C_2H_2) was dosed while heating the substrate at high temperature (above 600 °C), and the result was a quite low carbon uptake together with a breakdown of the layer, visible by a strong diffusion of Sr through the PZT layer. A second series of experiments started by depositing directly carbon on PZT/SRO/STO(001) from an electron bombardment evaporator. Carbon uptake was visible in this case, but the C 1s peak was broad, being a superposition of carbon in a wide range of chemical environments. Annealing the layers yielded to a narrowing of the C 1s and a clear angle dependence was observed in NEXAFS, but the main problem was still the diffusion of Sr onto the PZT layer. Consequently, a third series of samples were prepared by PLD deposition directly on a Pt(001) single crystal (Goodfellow). Prior to the deposition, the crystal was heated at 800 °C in 10^{-4} Pa oxygen, then annealed for about one hour with oxygen pumped down. The conditions for PLD deposition are described in grater detail in Refs. [13,15]. The experiments on these PZT/Pt(001) layers are those described in this paper. Once introduced in the experimental chamber, the layers were annealed in oxygen atmosphere (5×10^{-3} Pa) to remove all contaminants, following the procedure described in Ref [11]. Broad low energy electron diffraction patterns (LEED) were visible. The photoemission spectra obtained for the as introduced layer and following several annealing steps are described in SI. The result is that after two series of annealing in O_2 (5×10^{-3} Pa) stable Pb/(Ti + Zr) and O/(Ti + Zr) ratio are obtained from photoemission. A first carbon deposition was performed at 400 °C, then the

layer was annealed, and at 550 °C carbon was completely desorbed. These time-resolved experiments are represented in Figure 2 and in Figure S16. Thus, the layer was heated at 550 °C, C evaporation was initiated, and the temperature was decreased up to the onset of carbon sticking on the surface (at 510 °C, see Figure S17). This was the second deposition. The third and fourth depositions proceeded also at 510 °C (Figures S18 and S19). All depositions were characterized by photoelectron spectroscopy, while depositions 2 to 4 were analyzed also by near-edge X-ray absorption fine structure (NEXAFS) at the carbon K-edge, at variables angles of incidence.

Post-experiment manipulations: After the fourth deposition, the C/PZT layer was removed by Ar^+ sputtering, then the Pt(001) was prepared by cycles of sputtering and annealing. Sharp LEED spots were observed and no contamination was recorded. Afterwards, a Gr layer was synthesized on Pt(001) by CVD starting with C_2H_2. The C 1s spectrum of this Gr layer was used to calibrate the carbon amount on PZT layers. Cross checks with other experiments performed in the same setup with Gr/Ir(111) grown by CVD or by C deposition starting with the same electron bombardment evaporator were performed (these last layers were also characterized by scanning tunneling microscopy). The accuracy of the C 1s signal attributed to a graphene single layer is estimated to be reliable within ± 7.5 %.

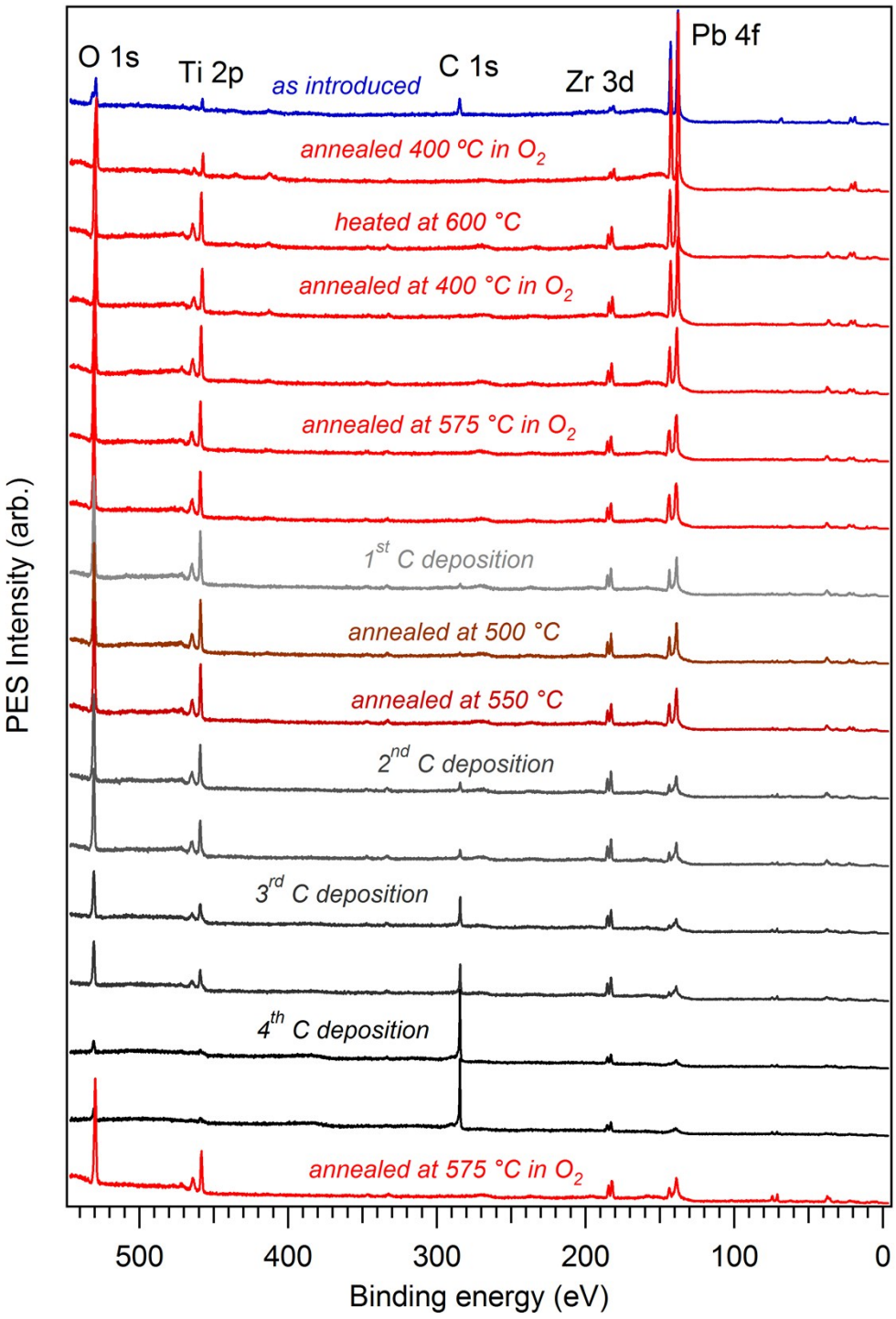

Figure S1. Overviews (survey scans) of photoelectron spectra from all layers and depositions discussed in this Letter.

SI-2. XPS analysis of the PZT samples prior to C deposition

As a general strategy, always the minimum numbers of components were used in the deconvolution.

Table S1. Binding energies and compositions extracted from the XPS data, for all core levels (Pb 4f, Zr 3d, Ti 2p, O 1s), and for all components used in the fit, for the "as introduced" sample and after different treatments. For the Pb 4f spectrum, the component at the lowest binding energy was not considered, since it belongs to some residual metal Pb on the surface. The component at 132-133 eV is in fact an Auger peak (Pb N_7VV) and also was not considered in the composition determination. The integral intensities were normalized with the photoionization cross section (2.142 Mb for Pb 4f at $h\nu$ = 260 eV, 4.716 for Zr 3d at $h\nu$ = 260 eV, 1.203 for Ti 2p at $h\nu$ = 600 eV, 0.412 for O 1s at $h\nu$ = 600 eV) and a further correction of I(260 eV)/I(600 eV) = 2.31 was considered from the variation of the synchrotron beam intensity at different photon energies.

Sample	comp.	Core level binding energies (eV)				Composition	
		Pb $4f_{7/2}$	Zr $3d_{5/2}$	Ti $2p_{3/2}$	O 1s		
"as introduced"	C1	136.355	181.151	457.713	529.470	Pb/(Zr+Ti)	5.383
	C2	137.923	182.041	458.392	530.840	O/(Zr+Ti)	4.321
	C3	138.626			531.770	Zr/(Zr+Ti)	0.534
First O_2 treatment. 400 °C	C1	136.626	180.937	457.541	529.107	Pb/(Zr+Ti)	5.427
	C2	137.726	181.596	458.651	529.928	O/(Zr+Ti)	7.543
	C3	138.367			530.979	Zr/(Zr+Ti)	0.419
	C4	132.468					
Annealed. 600 °C	C1	136.923	182.388	458.403	530.072	Pb/(Zr+Ti)	1.376
	C2	138.416	182.325	458.832	531.410	O/(Zr+Ti)	3.942
	C3	138.761				Zr/(Zr+Ti)	0.474
	C4	133.274					
Second O_2 treatment. 400 °C	C1	136.485	181.299	457.822	529.578	Pb/(Zr+Ti)	1.535
	C2	138.414	182.046	458.230	531.151	O/(Zr+Ti)	4.443
	C3	137.885				Zr/(Zr+Ti)	0.486
	C4	132.730					
Short anneal. 575 °C	C1	137.119	182.066	458.909	530.306	Pb/(Zr+Ti)	0.568
	C2	139.152	182.731	458.389	531.861	O/(Zr+Ti)	2.924
	C3	138.437				Zr/(Zr+Ti)	0.630
	C4	133.694					

Pb 4f spectra

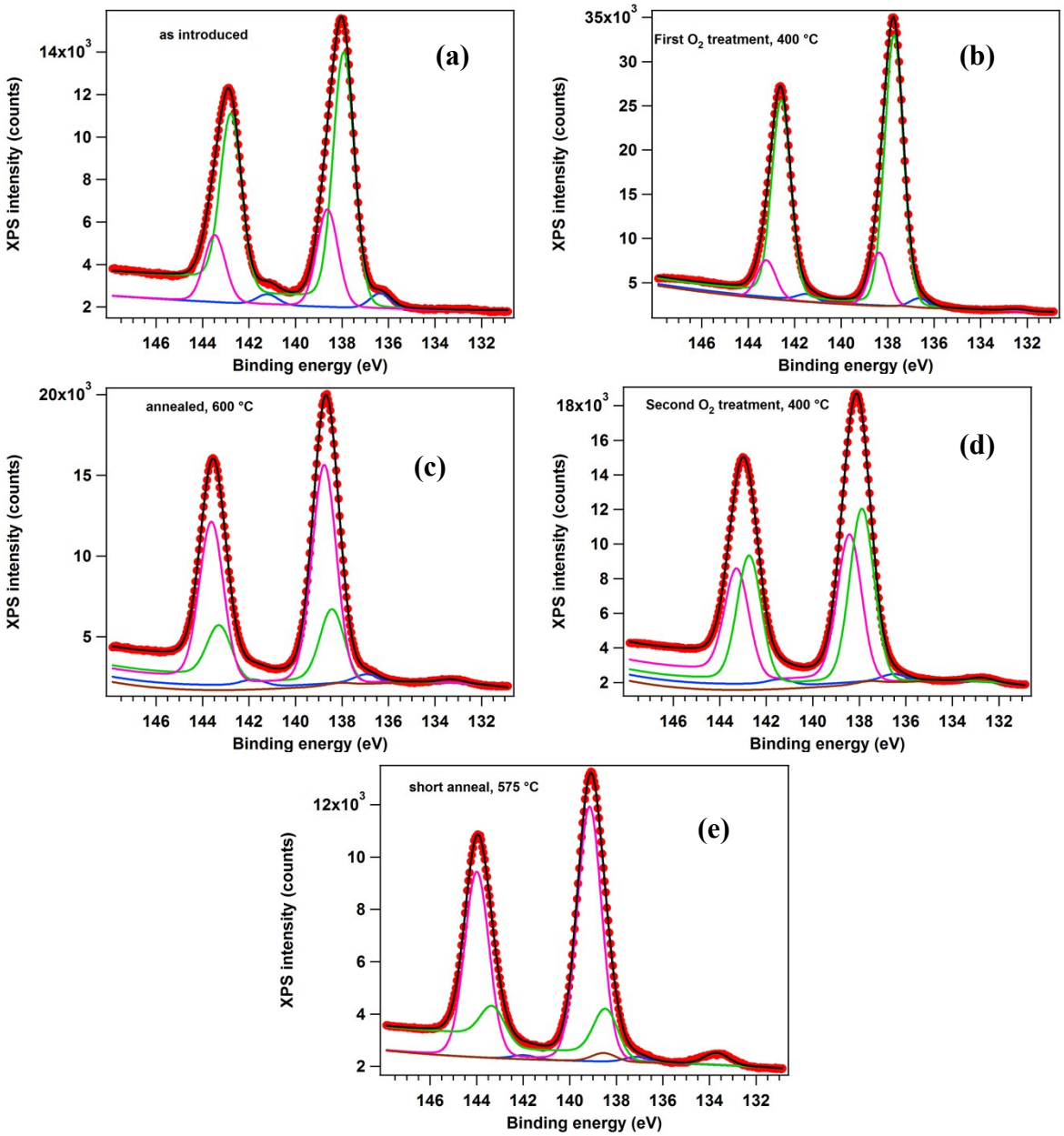

Figure S2. XPS Spectra for Pb 4f core levels, for the sample: (a) as introduced; (b) after first O_2 treatment, 400 ºC; (c) annealed, 600 ºC; (d) after second O_2, la 400 ºC; (e) short anneal, 575 ºC. The red circles represent the experimental data, the black line is the fit and the color lines are each separate component, with parameters listed in Table S1: C1, blue; C2, green; C3, magenta; C4, brown.

Zr 3d spectra

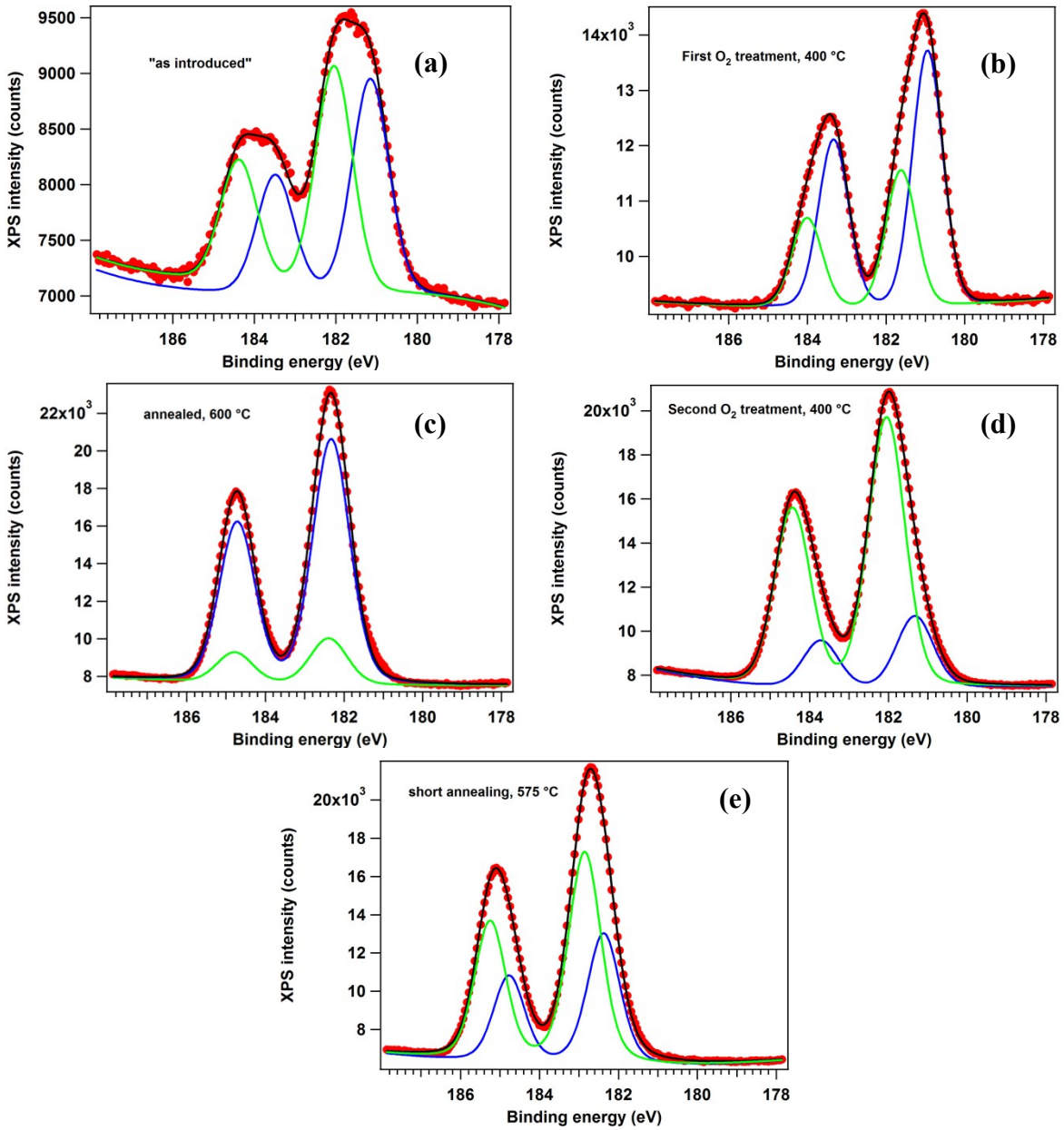

Figure S3. XPS Spectra for Zr 3d core level, for the sample: (a) as introduced; (b) after first O_2 treatment, 400 ºC; (c) annealed, 600 ºC; (d) after second O_2, la 400 ºC; (e) short anneal, 575 ºC. The red circles represent the experimental data, the black line is the fit and the color lines are each separate component, with parameters listed in Table S1: C1, blue; C2, green.

Ti 2p spectra

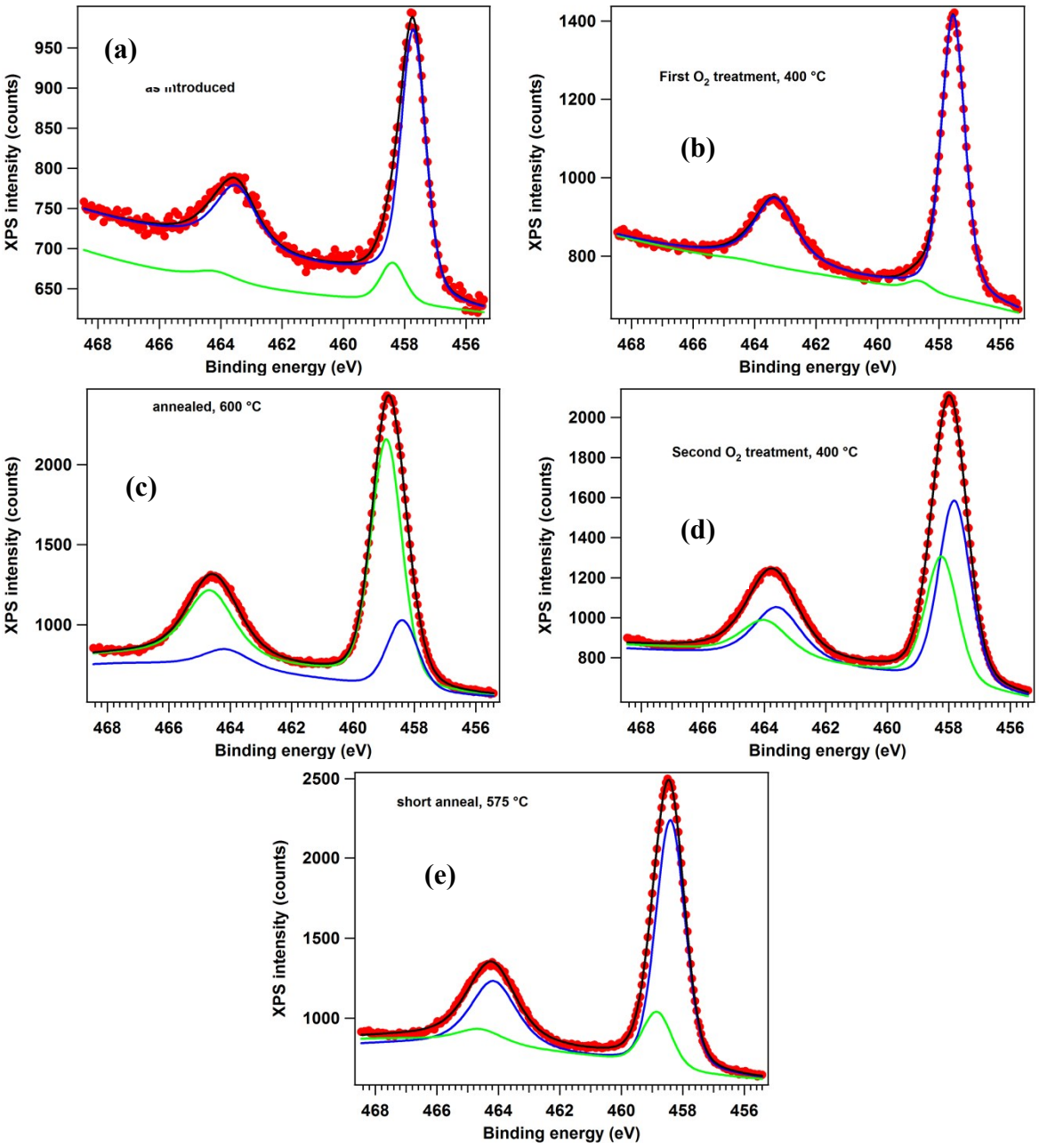

Figure S4. XPS Spectra for Ti 2p core level, for the sample: (a) as introduced; (b) after first O_2 treatment, 400 ºC; (c) annealed, 600 ºC; (d) after second O_2, la 400 ºC; (e) short anneal, 575 ºC. The red circles represent the experimental data, the black line is the fit and the color lines are each separate component, with parameters listed in Table S1: C1, blue; C2, green.

O 1s spectra

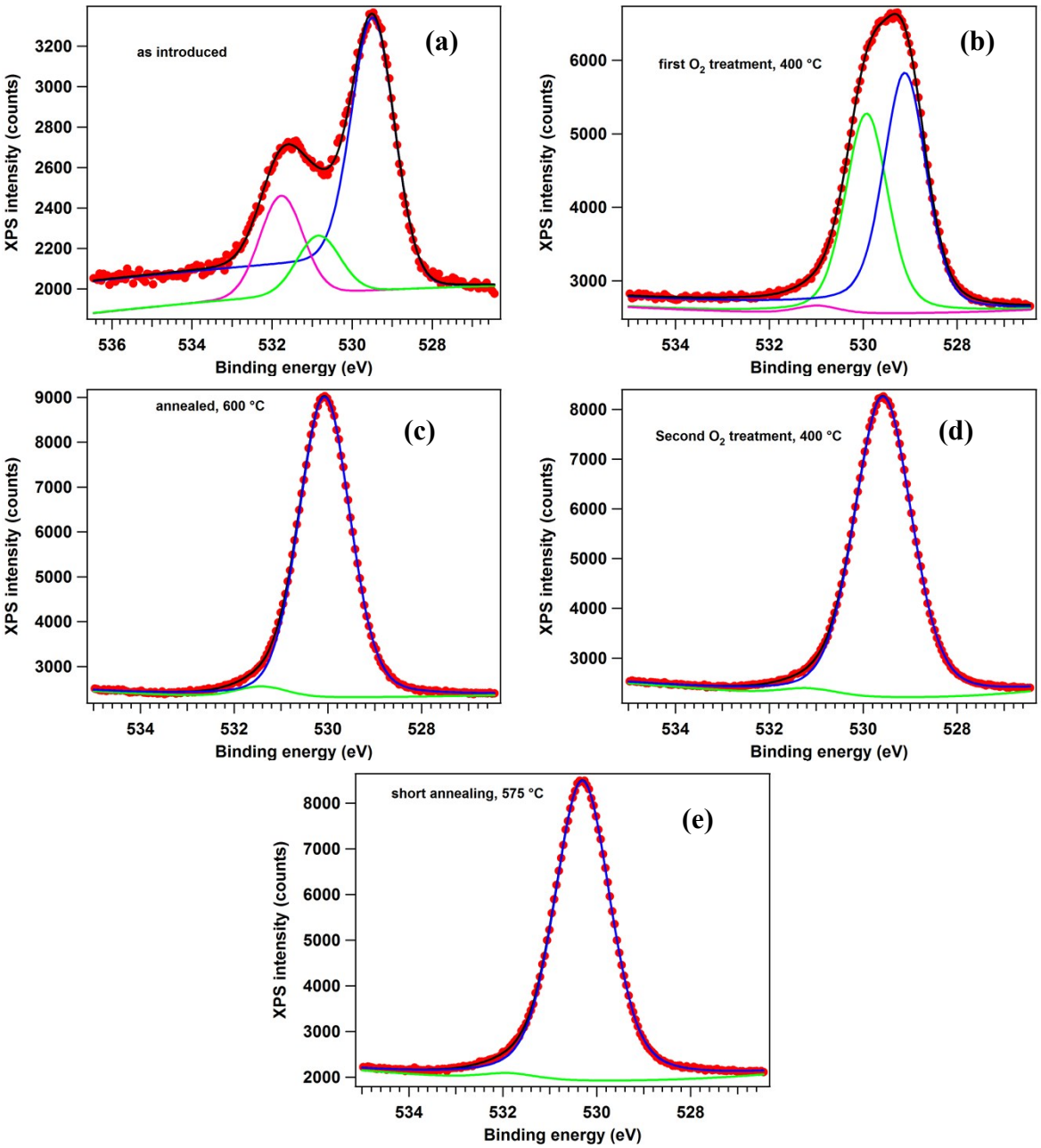

Figure S5. XPS Spectra for O 1s core level, for the sample: (a) as introduced; (b) after first O_2 treatment, 400 ºC; (c) annealed, 600 ºC; (d) after second O_2, la 400 ºC; (e) short anneal, 575 ºC. The red circles represent the experimental data, the black line is the fit and the color lines are each separate component, with parameters listed in Table S1: C1, blue; C2, green; C3, magenta.

C 1s spectra

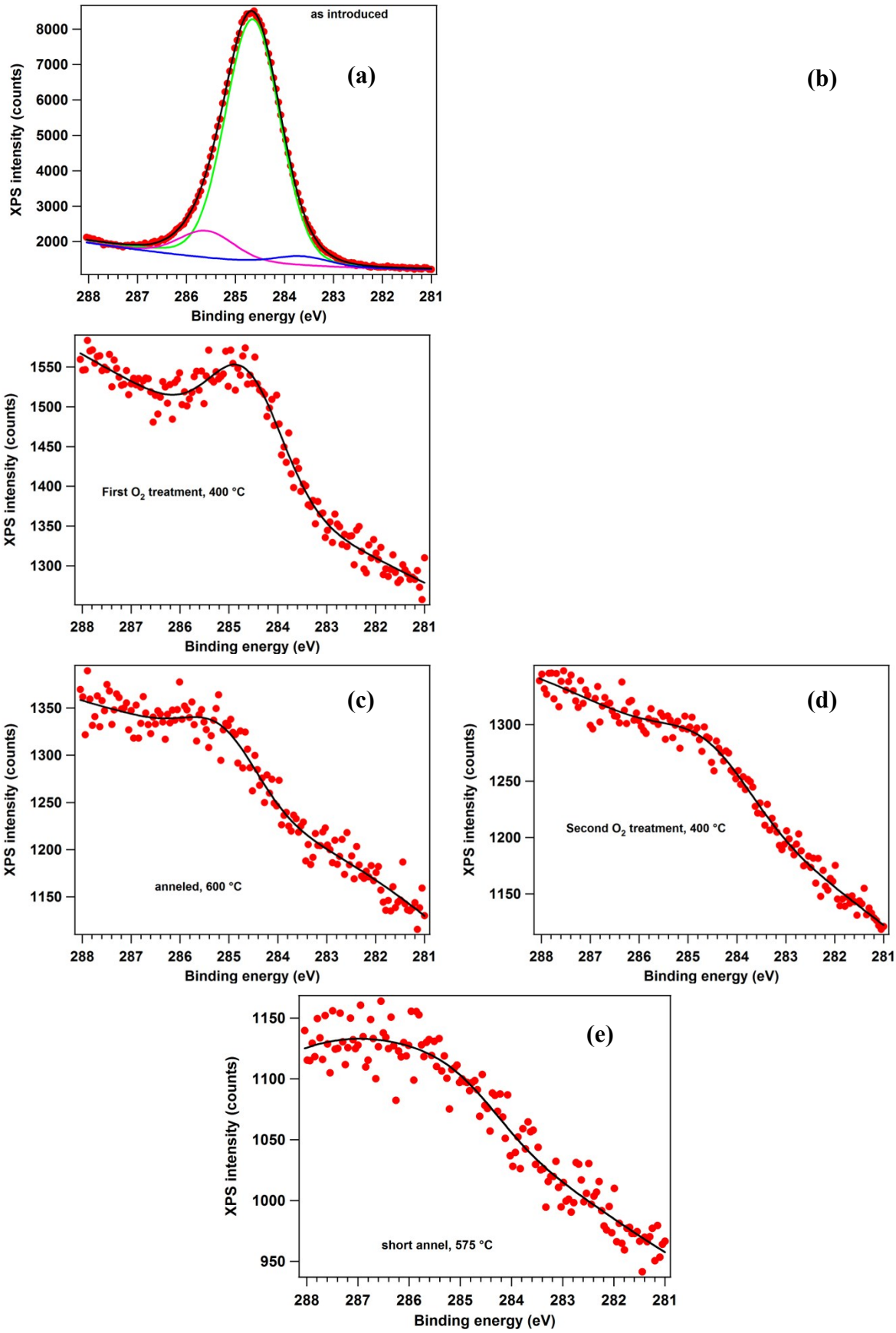
as introduced
(a)
(b)
XPS intensity (counts)
Binding energy (eV)
First O_2 treatment, 400 °C
(c)
anneled, 600 °C
(d)
Second O_2 treatment, 400 °C
(e)
short annel, 575 °C

Figure S6. XPS Spectra for C 1s core level, for the sample: (a) as introduced; (b) after first O_2 treatment, 400 ºC; (c) annealed, 600 ºC; (d) after second O_2, la 400 ºC; (e) short anneal, 575 ºC. The red circles represent the experimental data, the black line is the fit and the color lines are each separate component: C1, blue; C2, green; C3, magenta, in order of increasing binding energy for the „as introduced“ sample.

SI-3. XPS analysis of the PZT samples after C deposition

The small component of appearing in the Pb 4f at 132-133 eV was fitted with a singlet and was not considered at all in the composition determination. Also, Pb 4f components at low binding energies (136.7 – 137.2 eV) were not considered, being attributed to the ejection of metal Pb or Pb carbide.

Table S2. Binding energies and compositions extracted from XPS data, for all core levels (Pb 4f, Zr 3d, Ti 2p, O 1s) for samples after different C deposition and treatments. Same comments as in Table 1 apply for the Pb 4f components.

Sample	comp.	Core level binding energies (eV)				Composition	
		Pb $4f_{7/2}$	Zr $3d_{5/2}$	Ti $2p_{3/2}$	O 1s		
Deposition 1	C1	137.205	182.816	458.662	530.713	Pb/(Zr+Ti)	0.134
	C2	138.851	183.144	459.081	531.962	O/(Zr+Ti)	3.412
	C3	139.588	182.048	459.495		Zr/(Zr+Ti)	0.492
Annealed. 500 °C	C1	137.145	182.031	458.626	530.608	Pb/(Zr+Ti)	0.307
	C2	138.831	182.914	459.038	531.773	O/(Zr+Ti)	3.362
	C3	139.468		459.436		Zr/(Zr+Ti)	0.484
Annealed. 550 °C	C1	137.144	181.924	458.654	530.615	Pb/(Zr+Ti)	0.411
	C2	138.754	182.912	459.072	531.806	O/(Zr+Ti)	3.507
	C3	139.459		459.473		Zr/(Zr+Ti)	0.491
Deposition 2	C1	136.747	182.97	457.904	530.770	Pb/(Zr+Ti)	0.036
	C2	138.866		458.995	531.954	O/(Zr+Ti)	2.993
	C3	139.336		459.452		Zr/(Zr+Ti)	0.515
	C4	138.083					
Deposition 3	C1	136.714	182.939	457.986	530.719	Pb/(Zr+Ti)	0.028
	C2	138.999		458.923	531.944	O/(Zr+Ti)	2.670
	C3	140.065		459.408		Zr/(Zr+Ti)	0.564
	C4	137.802		457.221			
Deposition 4	C1	136.670	183.01	457.661	530.77	Pb/(Zr+Ti)	0.005
	C2	139.021		458.837		O/(Zr+Ti)	2.537
	C3			459.433		Zr/(Zr+Ti)	0.632

Deposition 1

Pb 4f spectra

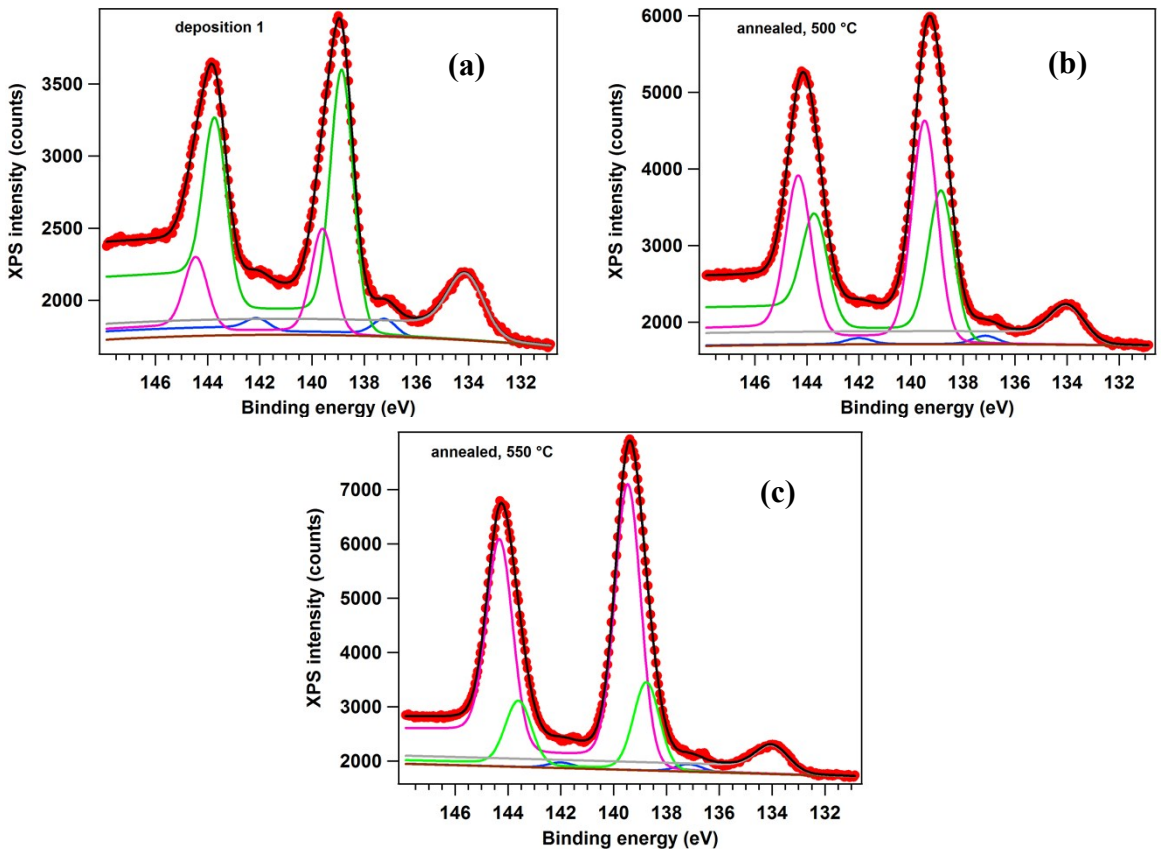

Figure S7. XPS Spectra for Pb 4f core level, for the sample: (a) after deposition 1; (b) annealed, 500 ºC; (c) annealed, 575 ºC. The red circles represent the experimental data, the black line is the fit and the color lines are each separate component, with parameters listed in Table S2: C1, blue; C2, green; C3, magenta; C4, brown.

Zr 3d spectra

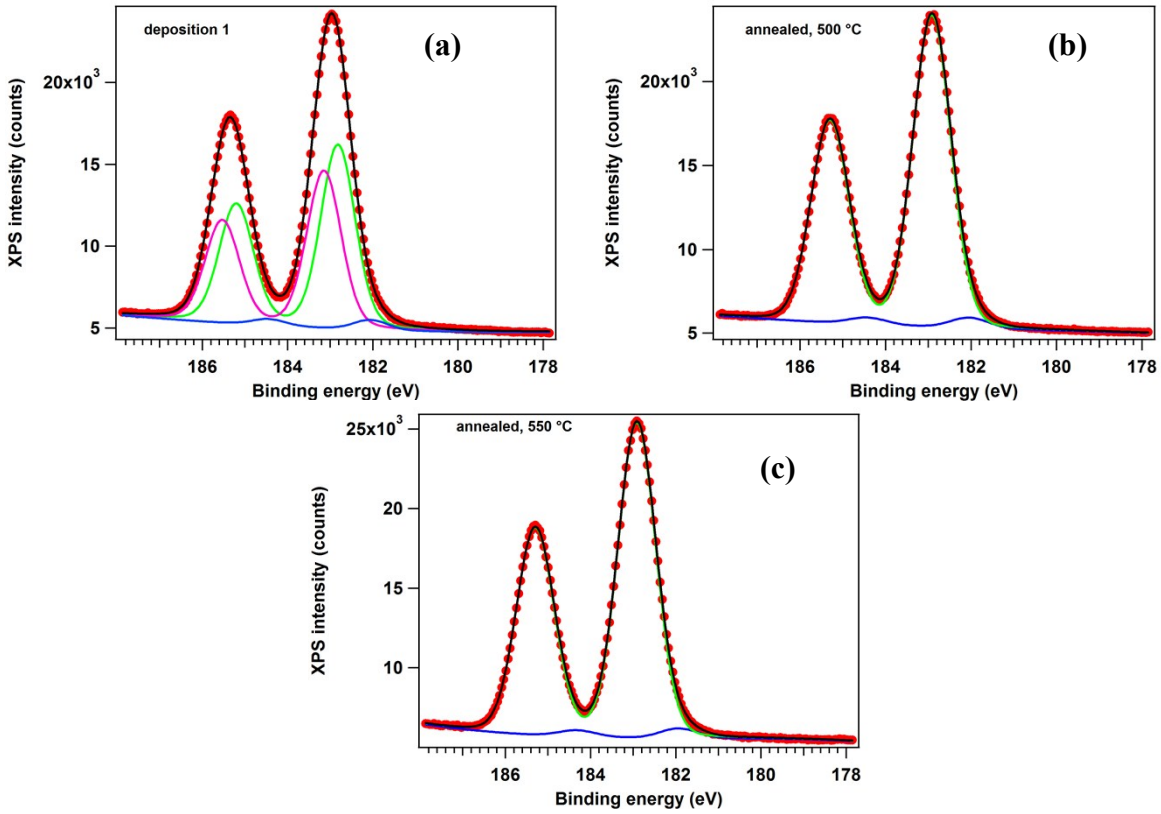

Figure S8. XPS Spectra for Zr 3d core level, for the sample: (a) deposition 1; (b) annealed, 500 ºC; (c) annealed, 575 ºC. The red circles represent the experimental data, the black line is the fit and the color lines are each separate component, with parameters listed in Table S2: C1, blue; C2, green; C3, magenta.

Ti 2p spectra

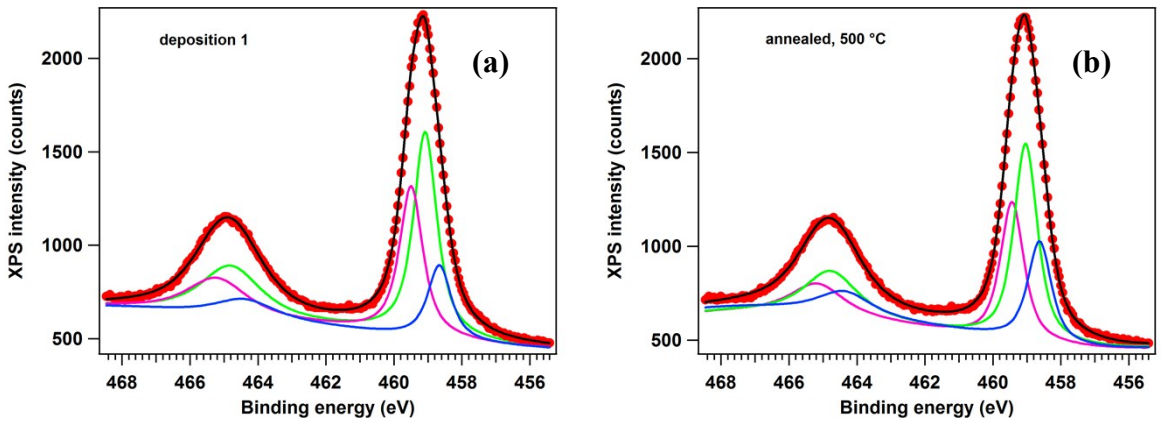

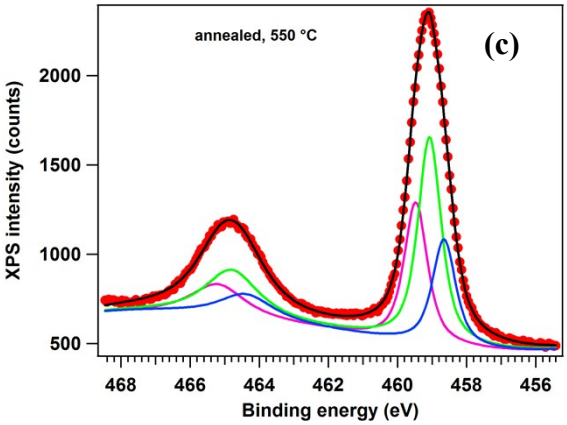

Figure S9. XPS Spectra for Ti 2p core level, for the sample: (a) deposition 1; (b) annealed, 500 ºC; (c) annealed, 575 ºC. The red circles represent the experimental data, the black line is the fit and the color lines are each separate component, with parameters listed in Table S2: C1, blue; C2, green; C3, magenta.

O 1s spectra

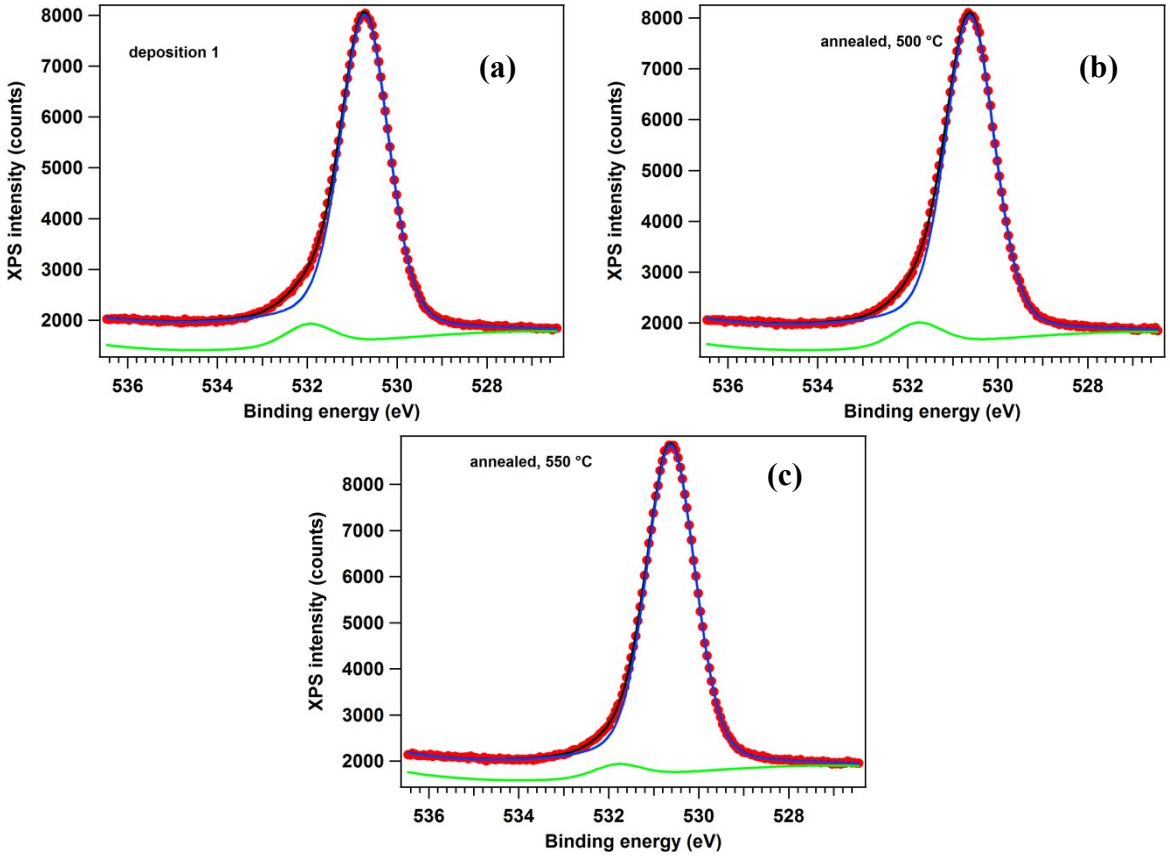

Figure S10. XPS Spectra for O 1s core level, for the sample: (a) after Carbon deposition 1; (b) annealed, 500 ºC; (c) annealed, 575 ºC. The red circles represent the experimental data, the black line is the fit and the color lines are each separate component, with parameters listed in Table S2: C1, blue; C2, green.

Deposition 2

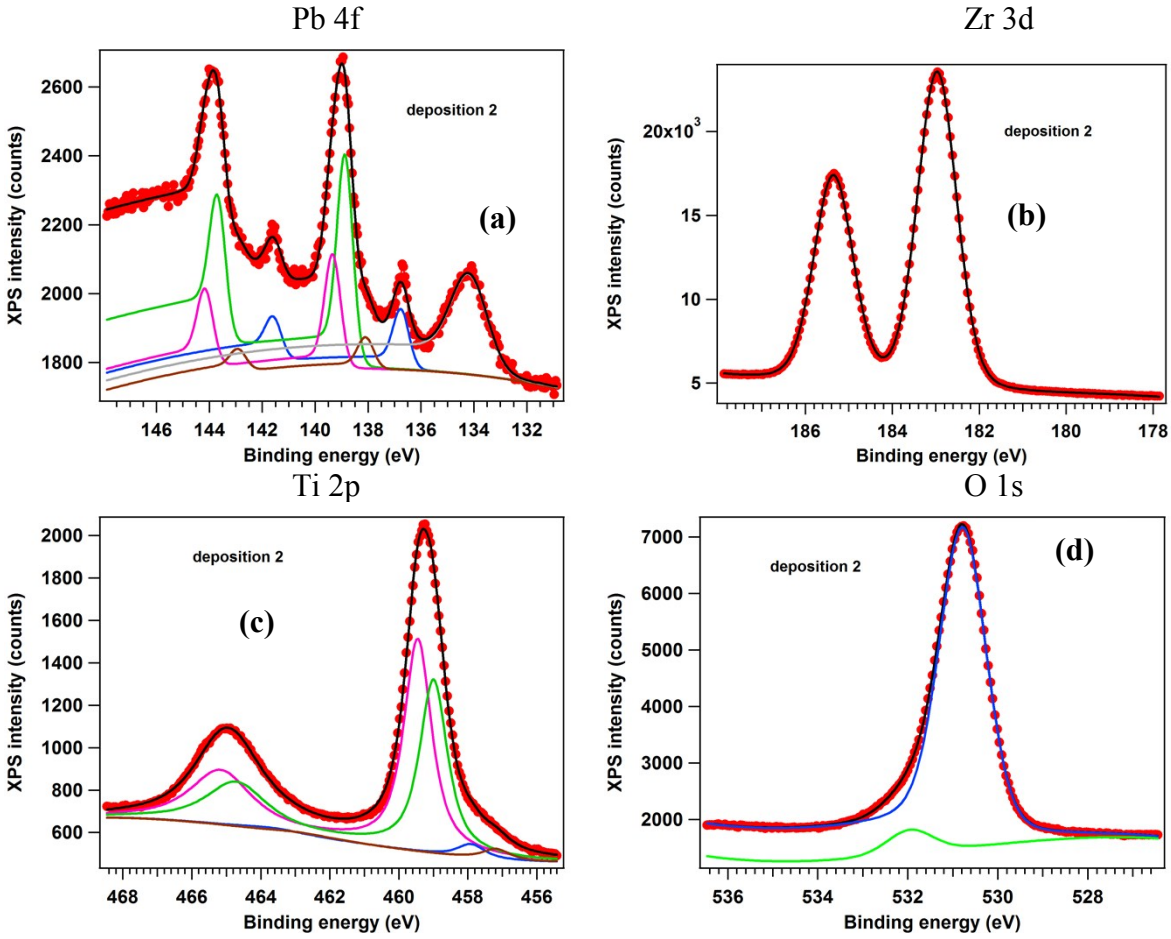

Figure S11. XPS Spectra after Carbon deposition 2, for all core levels: (a) Pb 4f; (b) Zr 3d; (c) Ti 2p; (d) O 1s. The red circles represent the experimental data, the black line is the fit and the color lines are each separate component, with parameters listed in Table S2: C1, blue; C2, green; C3, magenta; C4, brown.

Deposition 3

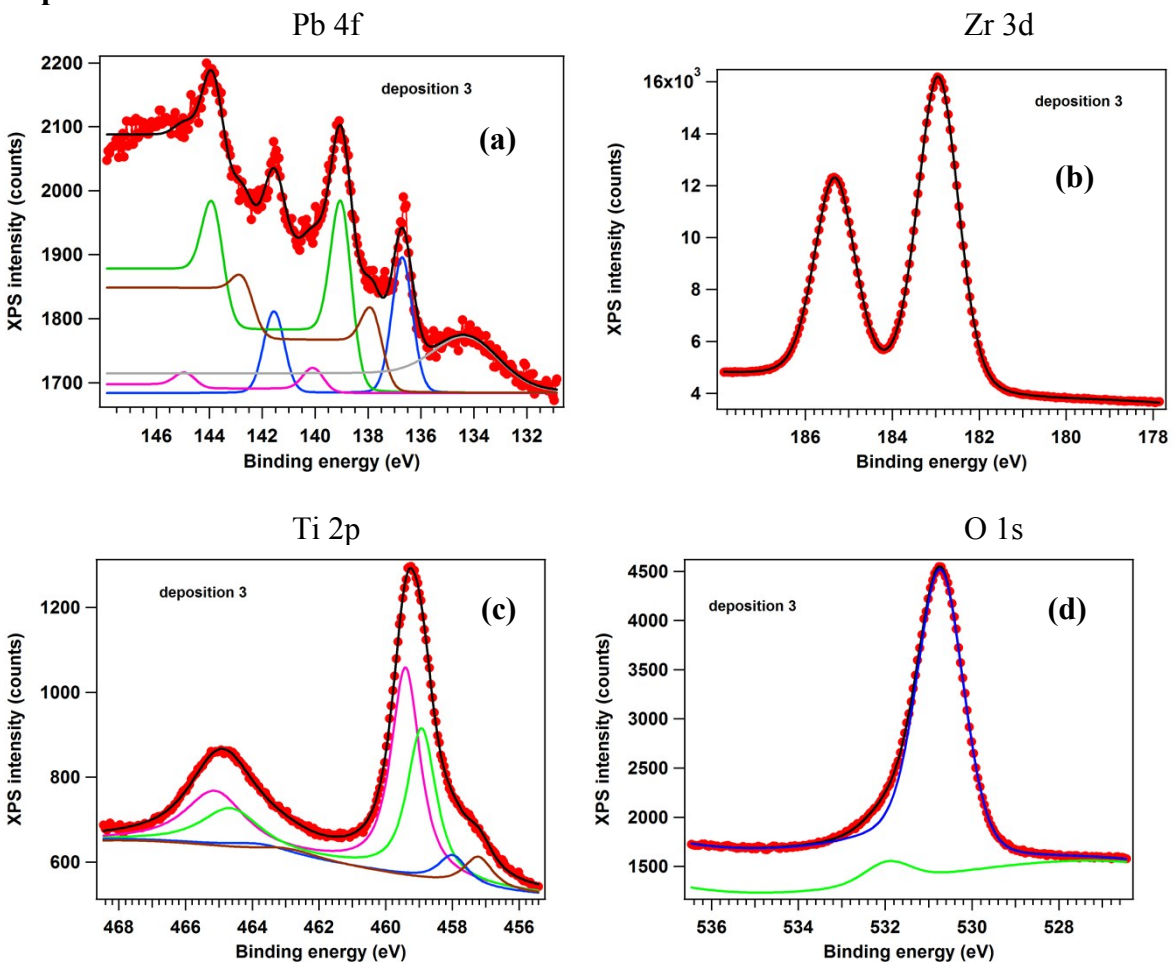

Figure S12. XPS Spectra after Carbon deposition 3, for all core levels: (a) Pb 4f; (b) Zr 3d; (c) Ti 2p; (d) O 1s. The red circles represent the experimental data, the black line is the fit and the color lines are each separate component, with parameters listed in Table S2: C1, blue; C2, green; C3, magenta; C4, brown.

Deposition 4

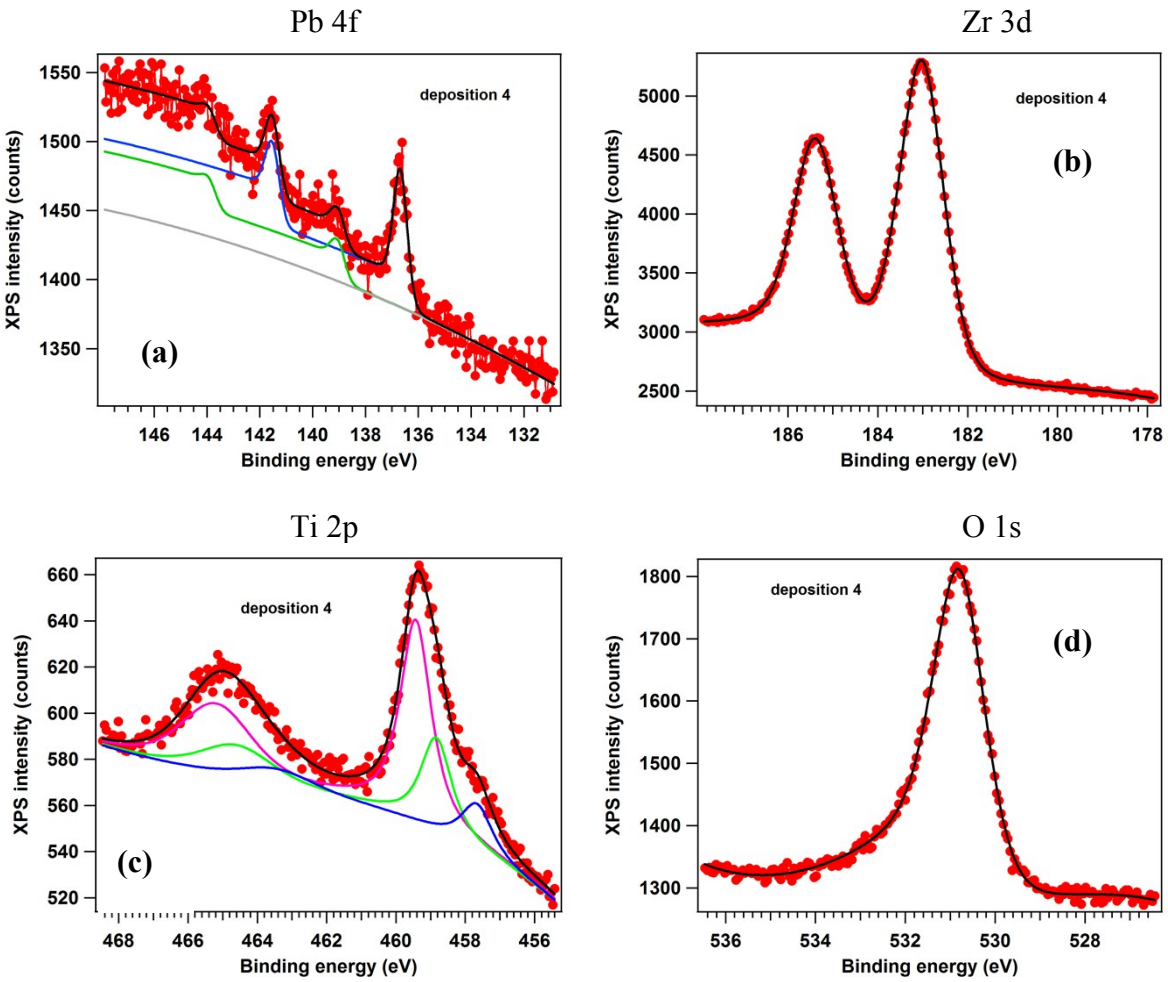

Figure S13. XPS Spectra after Carbon deposition 4, for all core levels: (a) Pb 4f; (b) Zr 3d; (c) Ti 2p; (d) O 1s. The red circles represent the experimental data, the black line is the fit and the color lines are each separate component; with parameters listed in Table S2: C1, blue; C2, green; C3, magenta.

Carbon 1s spectra for all depositions and for a graphene layer grown on Pt(001).

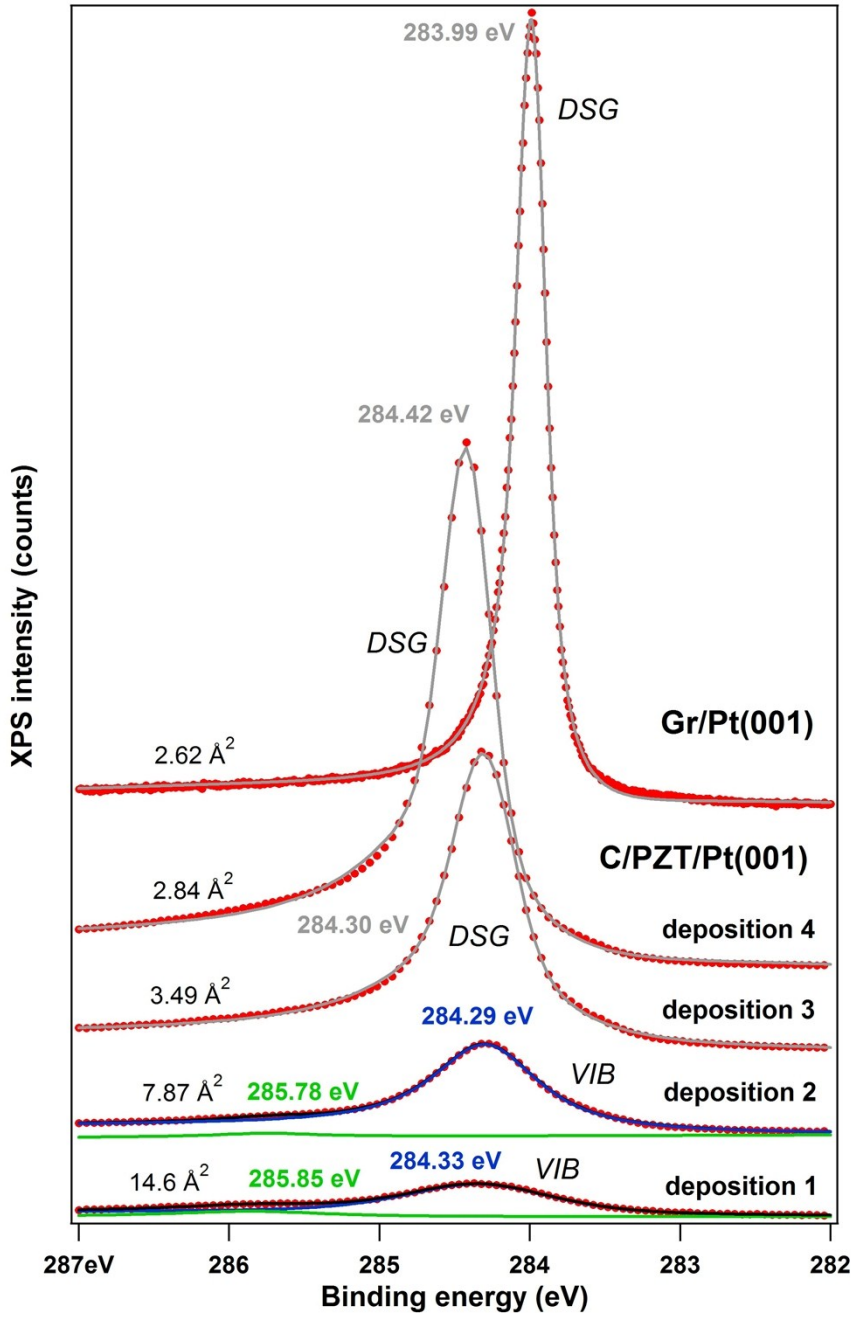

Figure S14. XPS Spectra for C1s core level after each Carbon deposition and for Graphene deposited on Pt(001) . The red circles represent the experimental data, the black line is the fit and the color lines are each separate component. VIB and DSG represent the fitting functions (Voigt with Integral Background and Doniach-Šunjić-Gauss, respectively).

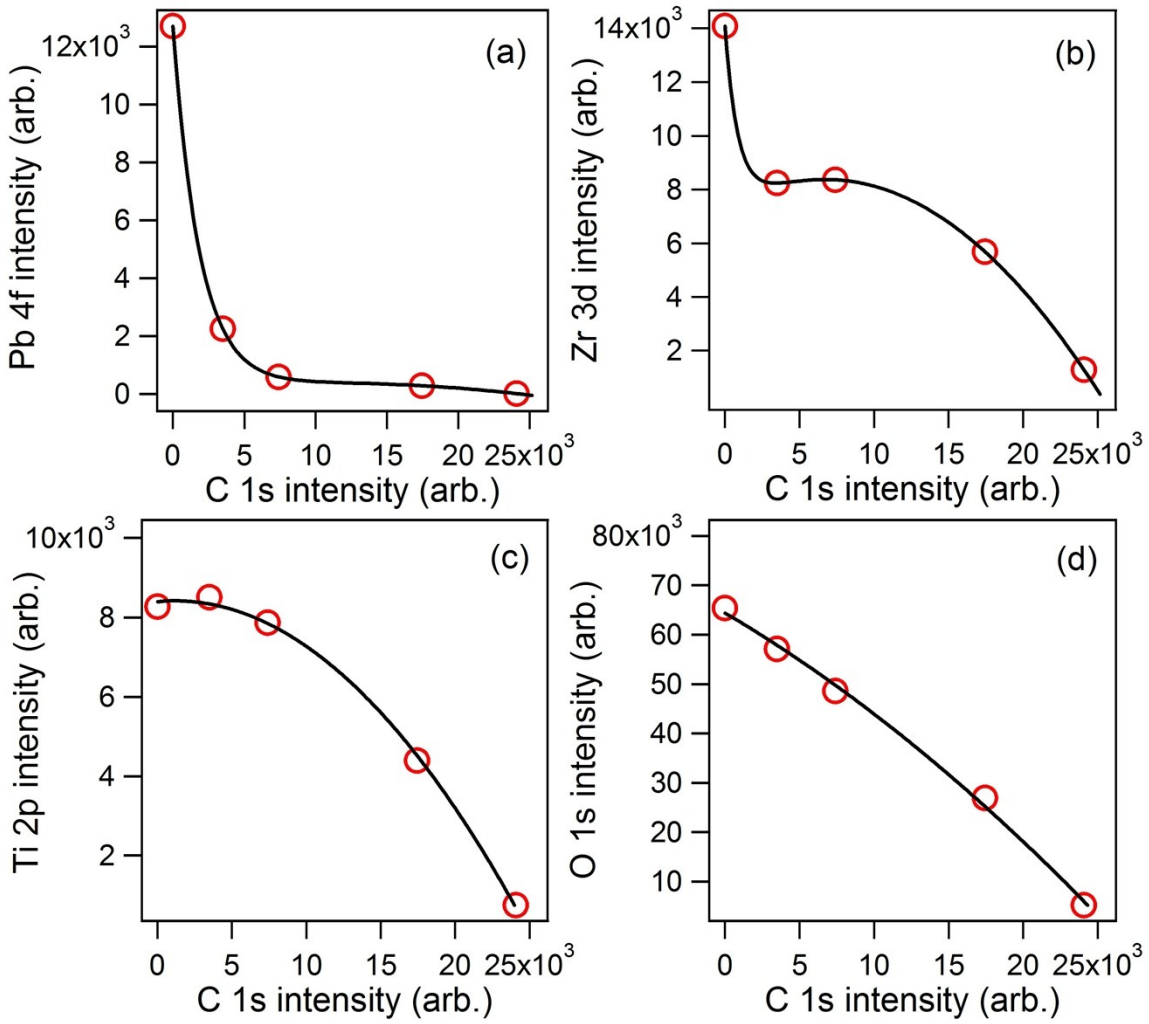

Figure S15. Evolution of total core levels intensities from the PZT layer (a) Pb 4f, (b) Zr 3d, (c) Ti 2p, (d) O 1s vs. the C 1s intensity. The full line is a fit by using the sum of an exponential decay and a parabola; its significance is rather an eye guide.

SI-4. Time resolved scans

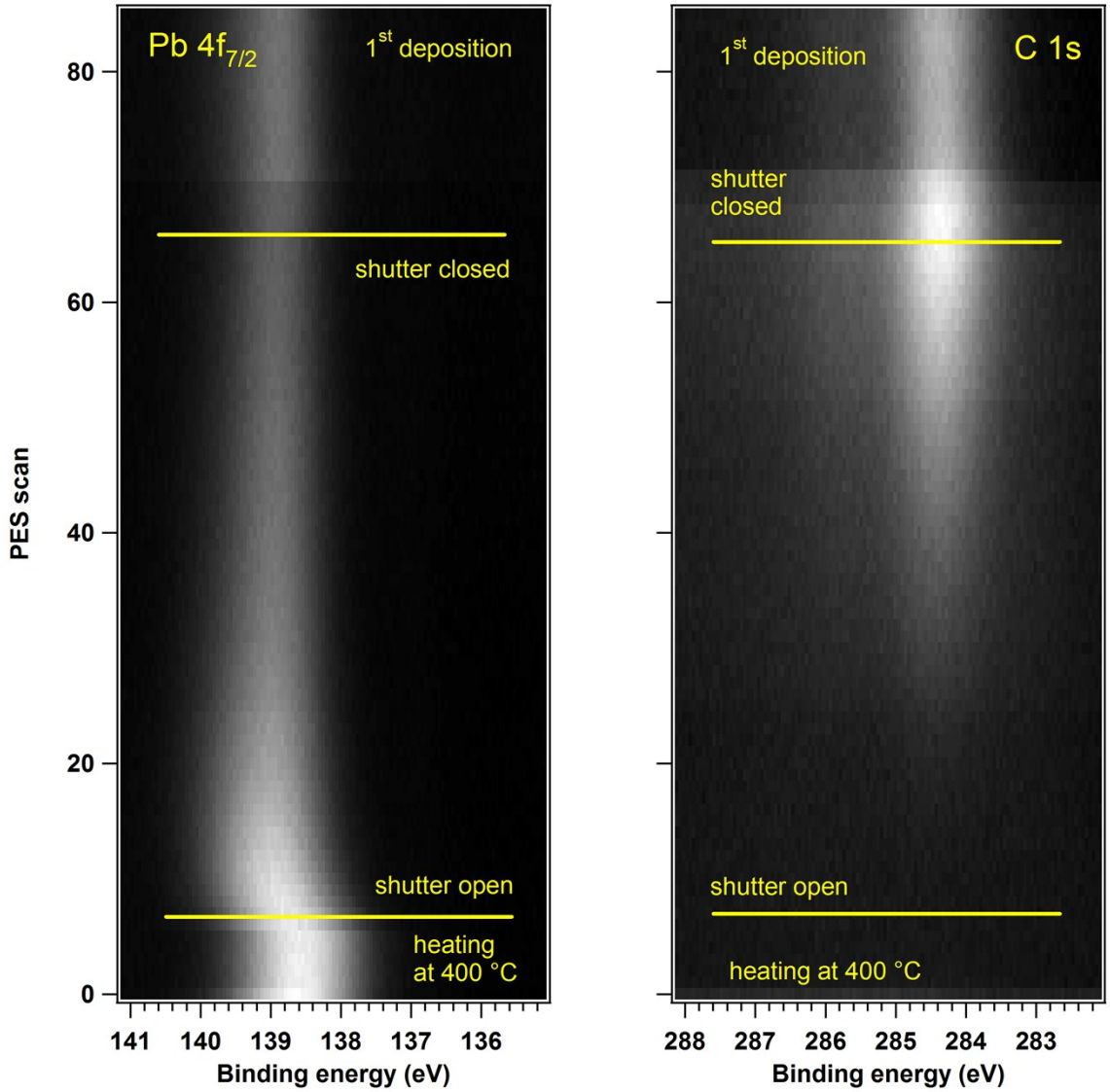

Figure S16. Time resolved photoemission (PES) spectra, represented in gray scale, with white corresponding to maximum intensity. (a) Pb $4f_{7/2}$ region and (b) C 1s region during the first carbon deposition at 400 °C. Note the shift of the Pb core level towards higher binding energy, when the shutter of the carbon evaporator is open. Most probably, this is an effect of light irradiation from the C source, which may produce electron emission from the layer and deplete the near surface electron sheet which compensates the depolarization field.

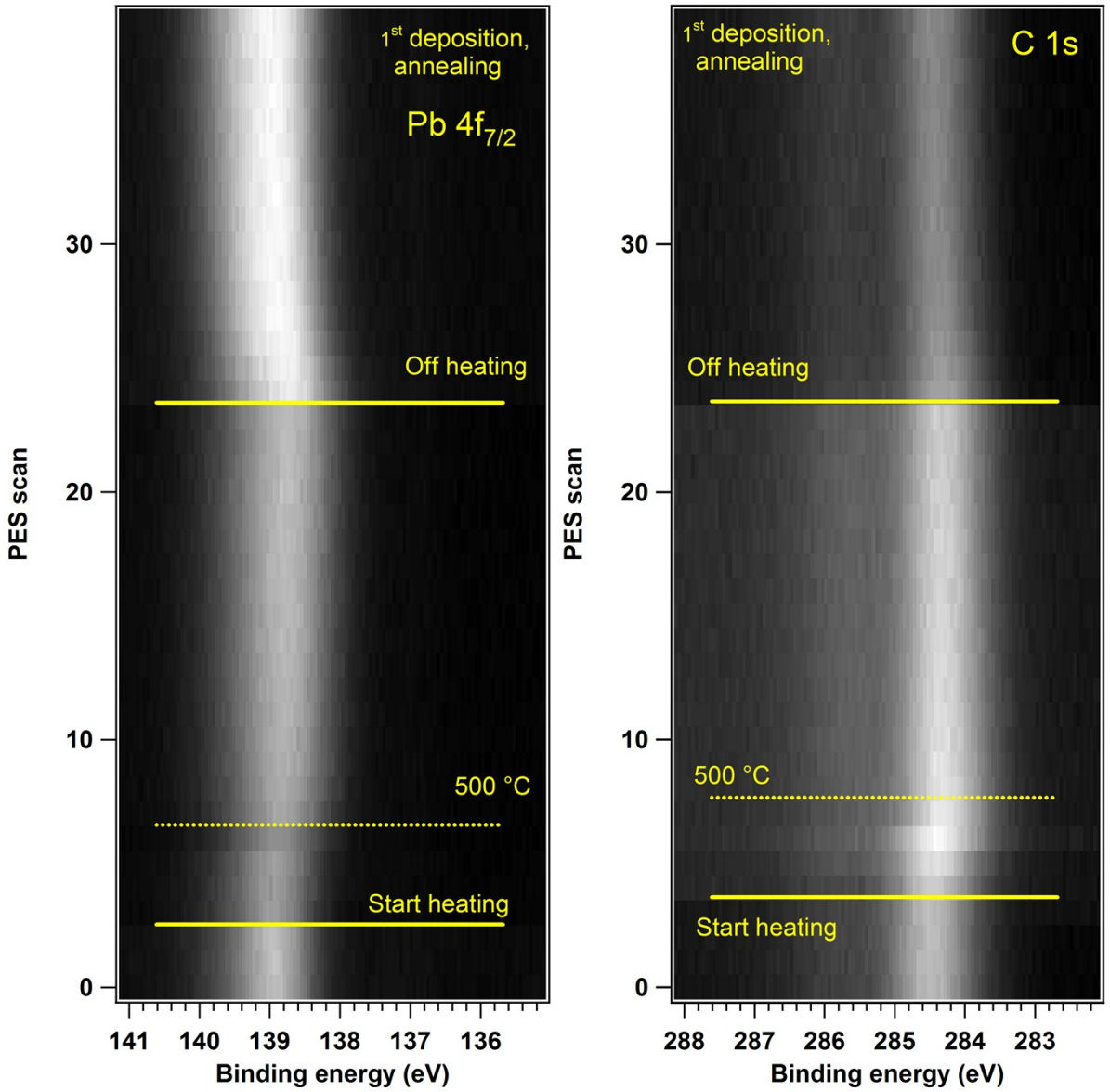

Figure S17. Time resolved PES scans from Pb $4f_{7/2}$ (left) and C 1s (right) during the annealing of the C layer obtained by the first deposition. At 500 °C substrate temperature, carbon starts to desorb whereas from the position of the Pb binding energy, the out-of-plane $P^{(+)}$ polarization decreases. Bright areas represent large intensities.

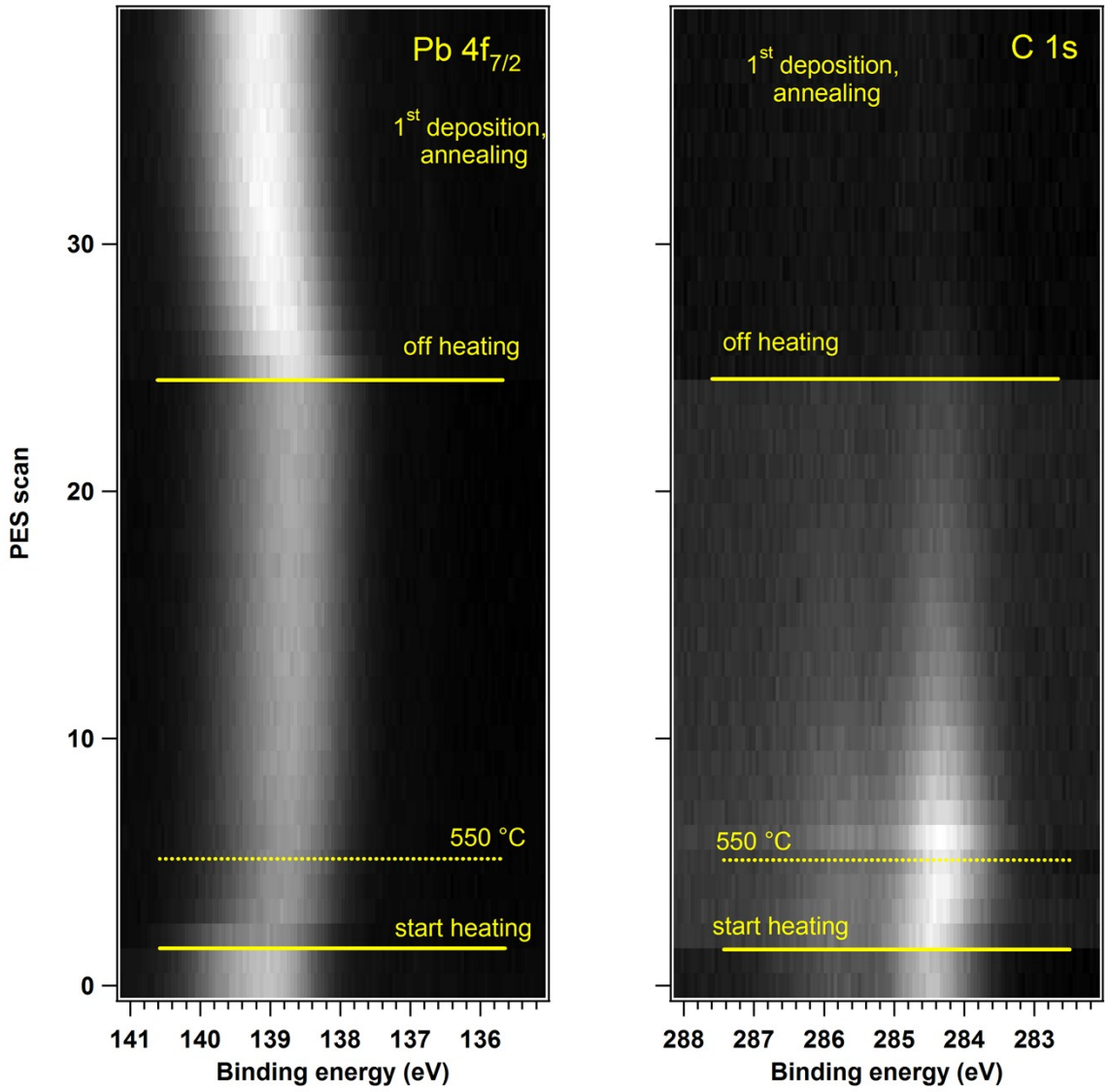

Figure S18. Time resolved PES scans from Pb $4f_{7/2}$ (left) and C 1s (right) during the second annealing at 550 °C of the C layer obtained by the first deposition. (a) Pb $4f_{7/2}$ region and (b) C 1s region. At this temperature, the polarization vanishes (Pb 4f shifts towards lower binding energies) and carbon is fully desorbed.

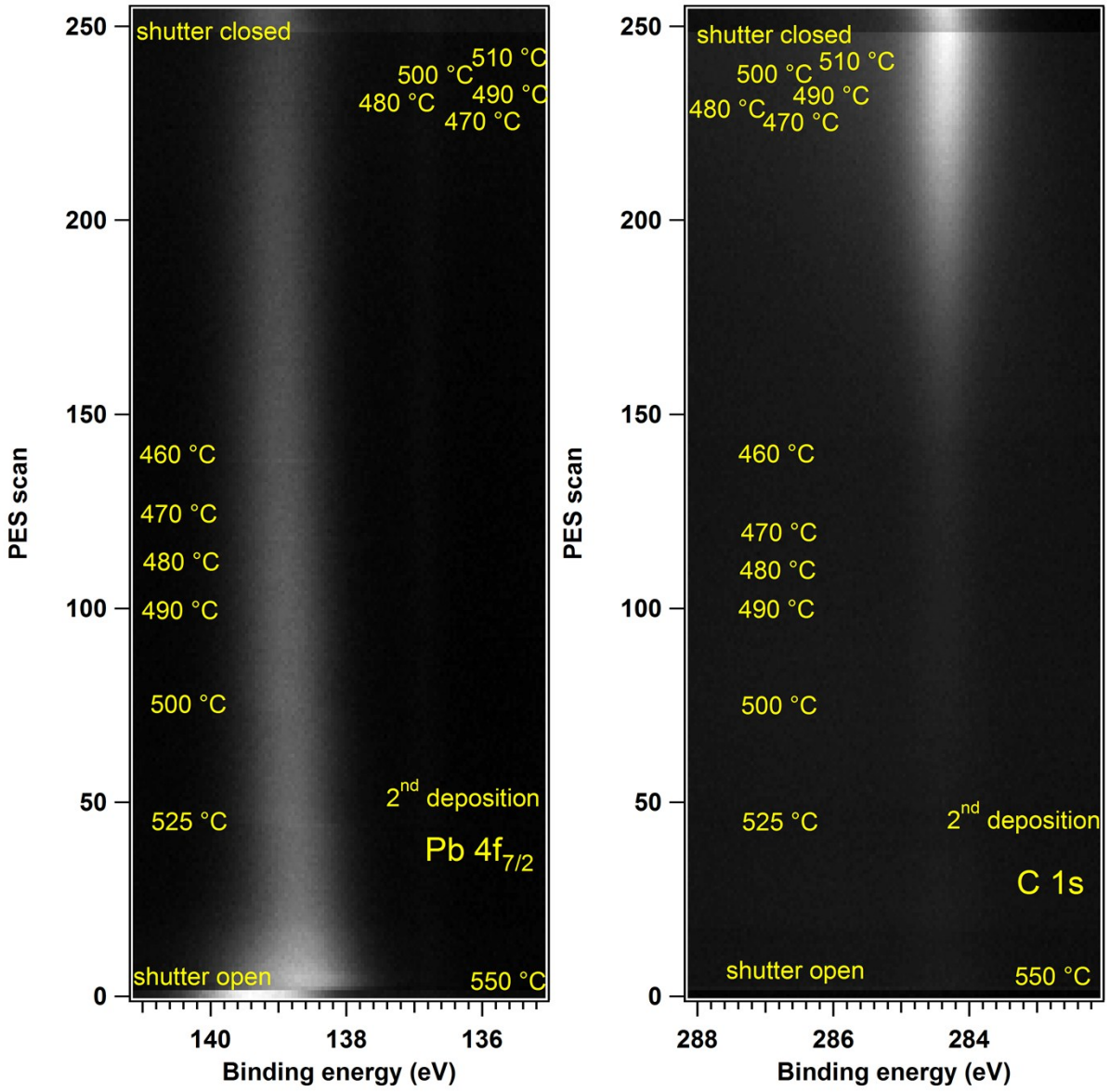

Figure S19. Time resolved PES scans during the second deposition process. It is visible that carbon starts to be deposited on the PZT film at temperatures around 460 °C.

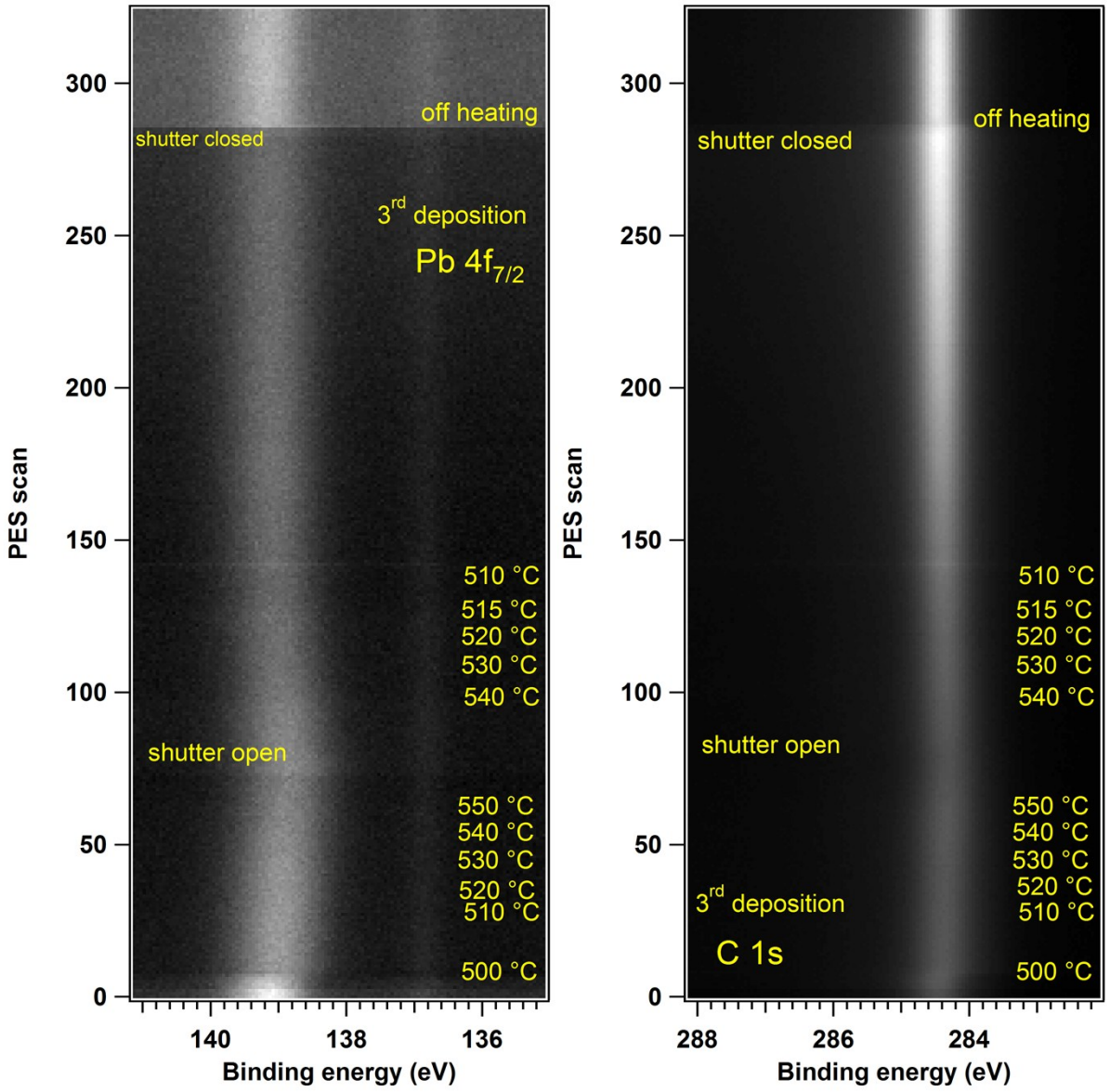

Figure S20. Time resolved PES scans during the third deposition. The sample was heated at 550 °C prior to the opening of the shutter of the evaporator. Then, the temperature was decreased progressively, and starting with 510 °C the C 1s signal starts to increase.

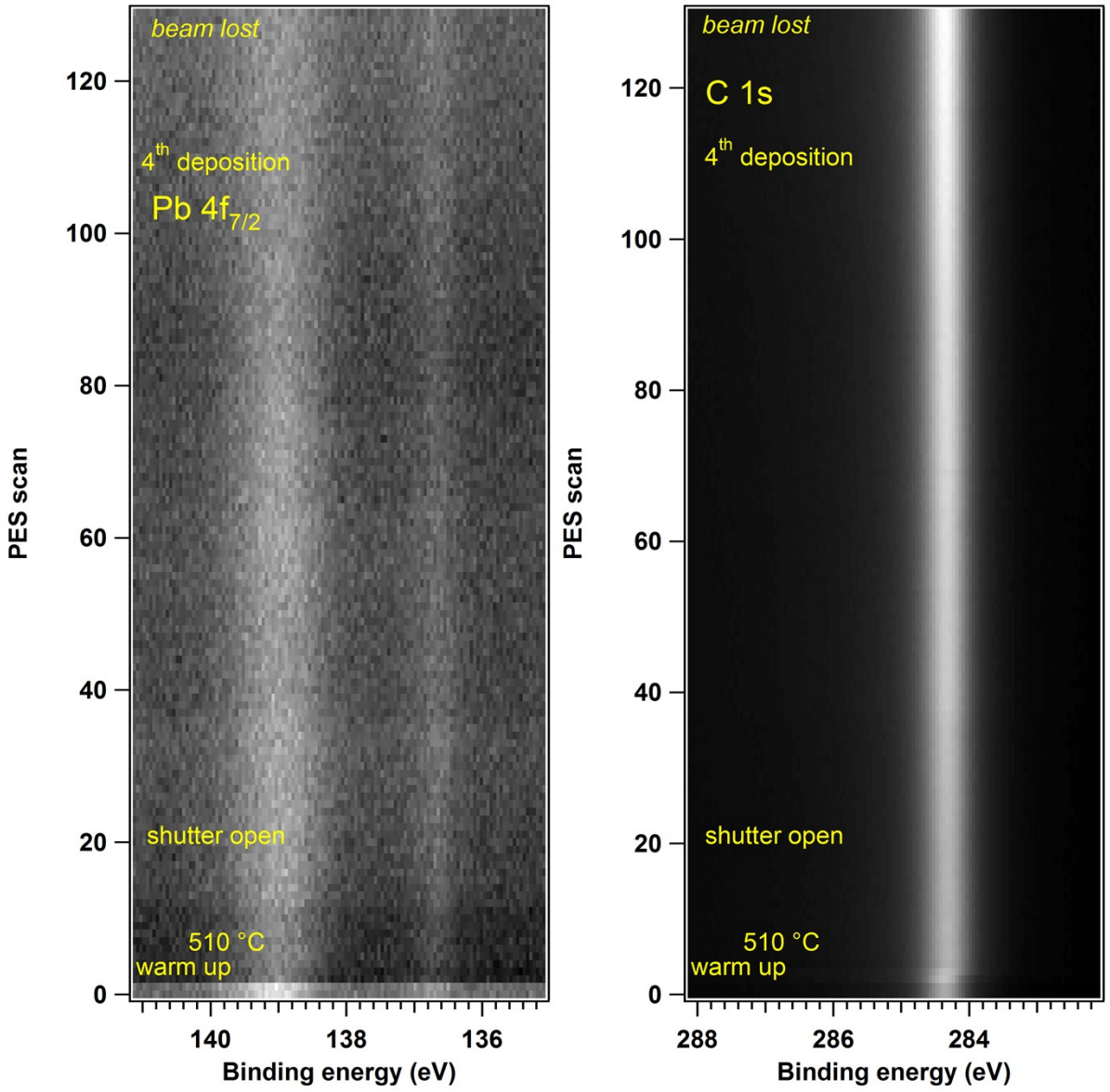

Figure S21. Time resolved PES scan during the fourth deposition. The whole process was performed at a temperature of 510 °C, derived from the previous processes.

SI-5. Carbon 1s Near-Edge Absorption Fine Structure from graphene synthesized on Pt(001)

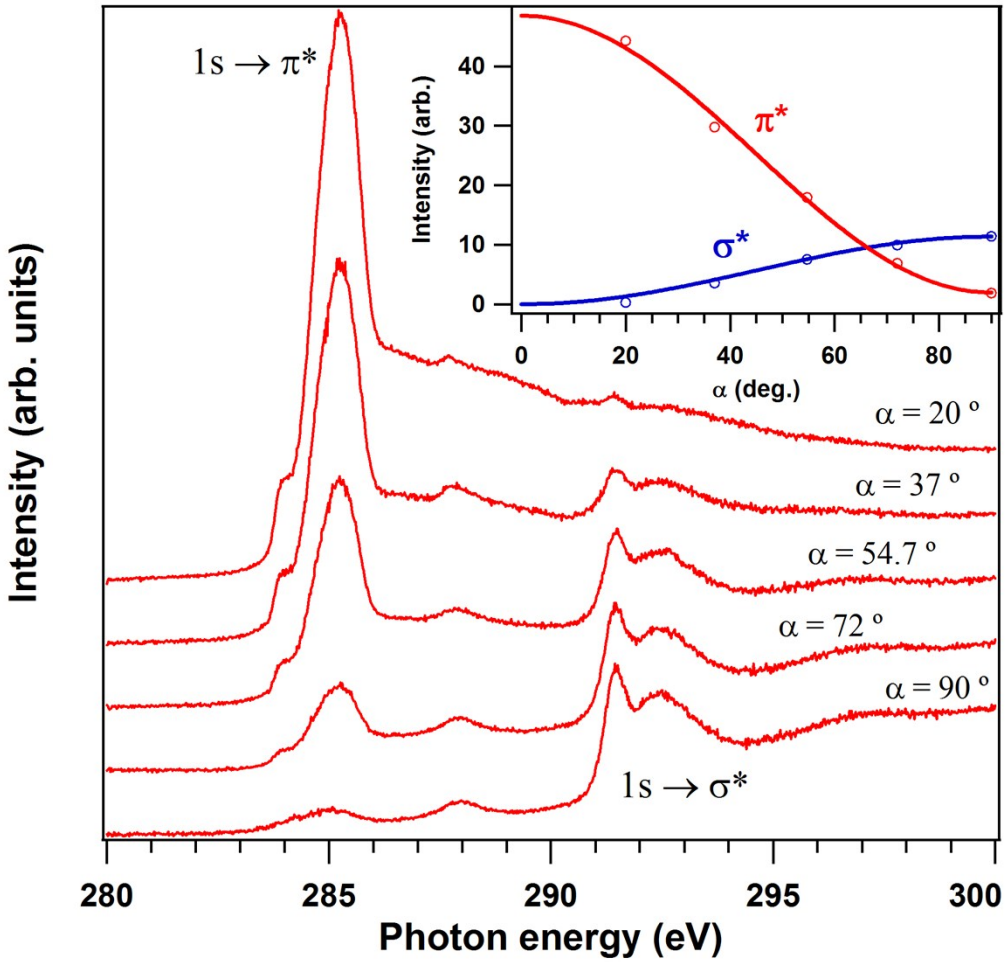

Figure S22. NEXAFS spectra at C K-edge for different incidence angles, in the case of Gr/Pt(001).